Biomicrofluidics

RESEARCH ARTICLE | MAY 27 2026

# Fabrication of cell-encapsulating hollow collagen microgel beads for engineered hollow tissues

Satona Abeta ; Aiki Hioki; Akari Masuda; Fabio Pizzeti; Filippo Rossi ; Kayoko Hirayama-Shoji ; Hiroaki Onoe



*Biomicrofluidics* 20, 034101 (2026)
https://doi.org/10.1063/5.0328551



**Connected Content**

A companion article has been published: Building better organ models, one collagen sphere at a time

Biomicrofluidics ARTICLE pubs.aip.org/aip/bmf

# Fabrication of cell-encapsulating hollow collagen microgel beads for engineered hollow tissues

Cite as: Biomicrofluidics **20**, 034101 (2026); doi: 10.1063/5.0328551
Submitted: 15 February 2026 · Accepted: 1 May 2026 ·
Published Online: 27 May 2026



Satona Abeta,[1] Aiki Hioki,[1] Akari Masuda,[1] Fabio Pizzeti,[2] Filippo Rossi,[2] Kayoko Hirayama-Shoji,[3] and Hiroaki Onoe[1,a)]

## AFFILIATIONS

[1]Department of Mechanical Engineering, Faculty of Science and Technology, Keio University, 3-14-1 Hiyoshi, Kohoku-ku, Yokohama 223-8522, Japan
[2]Department of Chemistry, Materials and Chemical Engineering "Giulio Natta," Politecnico di Milano, via Mancinelli 7, Milan 20131, Italy
[3]Department of Medical Genetics, Oslo University Hospital and University of Oslo, Oslo 0450, Norway

[a)]**Author to whom correspondence should be addressed:** onoe@mech.keio.ac.jp

## ABSTRACT

This paper presents fabrication process of cell-encapsulating hollow collagen microgel beads, which enables stable and large-scale production of hollow tissue models. The microgel beads feature a core–shell structure, with a liquid core containing a cell suspension and a collagen shell serving as a scaffold. Cells encapsulated within the core adhere to the inner collagen wall, leading to the formation of a defined hollow tissue. We demonstrated this by fabricating beads with encapsulated human umbilical vein endothelial cells, which successfully adhered to the inner surface. These results suggest that this approach geometrically guides the cells into a hollow structure, facilitating the engineered construction of hollow tissue architectures. The cell-encapsulating hollow collagen microgel beads are promising tools for reproducing pathological models of hollow organs for drug evaluation.





## I. INTRODUCTION

Three-dimensional tissues derived from pluripotent stem cells [e.g., embryonic stem cells (ESCs) and induced pluripotent stem cells (iPSCs)] through induced differentiation and self-organization[1–3] serve as promising tools for disease modeling and drug discovery.[4,5] For example, *in vitro* intestinal tissue for reproducing inflammatory bowel disease[6] and *in vitro* liver cancer tissue for evaluating drugs for cancer therapy[7] have been reported so far.

*In vitro* hollow tissues, which mimic organs such as the heart and stomach, are of particular interest because their structure is fundamental to their function. The chamber of the heart, for example, is essential for its role as a pump to circulate blood, while the cavity of the stomach is critical for containing and transporting nutrients.[8,9] Therefore, recreating these hollow architectures is vital for accurately modeling physiological functions and pathologies.[10,11] Although *in vitro* tissues are effective to understand the functions and disease mechanisms of organs in our body, their generation faces some challenges: conventional methods depend on cellular self-organization, a process that offers limited control over the final tissue size and architecture, particularly for creating consistent hollow geometries.[12,13] As an alternative to self-organization, tissue engineering approaches using microgel beads offer a higher degree of structural control.[14,15] Microfluidic devices enable the fabrication of cell-laden microgels from extracellular matrix (ECM)-based materials, which act as a scaffold to support three-dimensional tissue formation. This strategy has been successfully applied to engineer solid tissues, for instance, using collagen microgel beads for bone tissue construction,[16] and Matrigel-based microgel beads for glandular tissue formation.[17] However, the creation of ECM-based microgels with a stable, liquid-filled hollow core has remained a critical unmet challenge. Consequently, the engineered formation of hollow tissues within microgel scaffolds has not been achieved.

To address this gap, we propose a method for fabricating cell-encapsulating hollow collagen microgel beads using a sacrificial alginate gel template (Fig. 1). Our method produces core–shell microgel beads where the outer shell is composed of collagen,

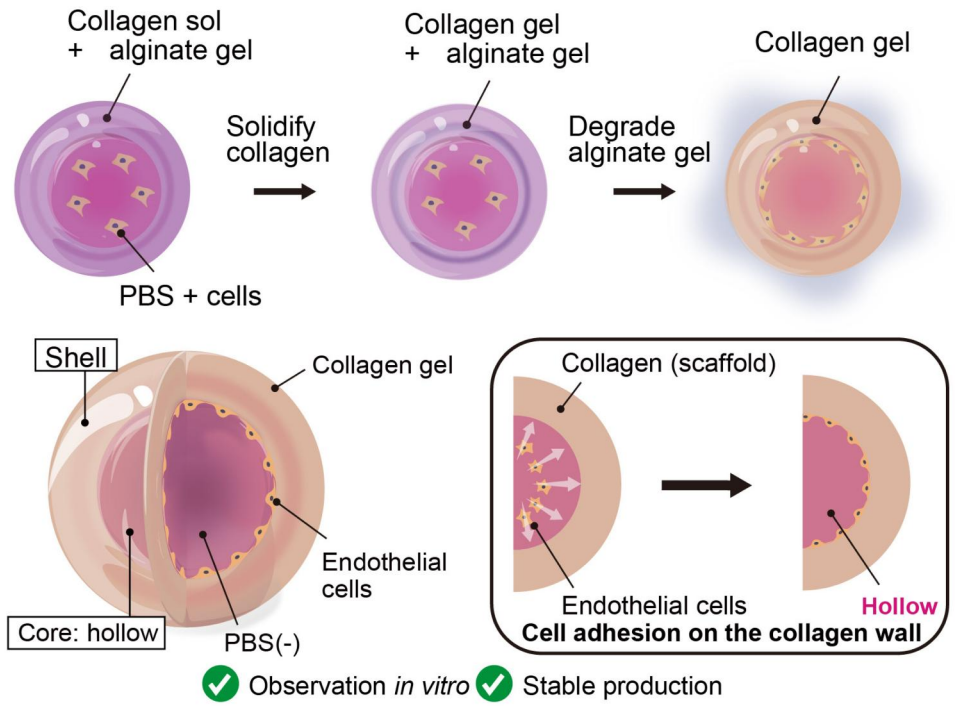


**FIG. 1.** Concept of our cell-encapsulating hollow collagen microgel beads. Our cell-encapsulating hollow collagen microgel beads are fabricated using the alginate template method. Cells encapsulated inside the beads adhere to the inner collagen wall, forming hollow structure.

providing a biocompatible scaffold,[18] while the inner core contains a cell suspension. This design directs the encapsulated cells to adhere to the inner wall of the collagen shell, thereby forming a chamber lined with cells. In this paper, we demonstrated the principle by encapsulating human umbilical vein endothelial cells (HUVECs). We confirm that the cells remain viable and adhere to the inner collagen scaffold to create the intended hollow architecture, offering a robust platform for engineering *in vitro* hollow tissue.

## II. EXPERIMENTAL

### A. Cell culture

Mouse fetal fibroblasts, NIH/3T3 cells (RCB2767, RIKEN) and Human Umbilical Vein Endothelial Cells, HUVECs (C-12200, PromoCell), were cultured. NIH/3T3 cells were maintained in Dulbecco's Modified Eagle Medium (DMEM) (SIGMA) supplemented with 10% Fetal Bovine Serum (FBS) (Corning) and 1% Penicillin–Streptomycin Solution (PS) (Sigma-Aldrich) at 37 °C under water-saturated 5% $CO_2$ atmosphere. HUVECs were maintained in Endothelial Basal Medium (PromoCell) supplemented with FBS at 37 °C and water-saturated 5% $CO_2$ atmosphere. Before becoming confluent, both cells were passaged using trypsin (Trypsin-EDTA, ThermoFisher).

### B. Preparation of fluorescent alginate

Alginate was chemically functionalized with Rhodamine B. The reaction involved three different steps, namely, the preparation of propargyl alginate and rhodamine-azide and finally, the covalent bond formation between the two through click chemistry. As far as the first step is concerned, alginic acid sodium salt (1 g, 1 eq.) is dissolved in 5 ml of water, and then propargylamine (0.125 g, 0.5 eq.) was added. Separately HOBt (0.313 g, 0.5 eq.) was dissolved in 2.5 ml of distilled water and 7.5 ml of $CH_3CN$. After dissolution, this was added dropwise to the alginate one. 1-Ethyl-3-(3-dimethylaminopropyl) carbodiimide (EDC) hydrochloride (0.444 g, 0.5 eq.) was added to the mixture, and the reaction has been let proceed for 24 h at room temperature. Purification step involved dialysis for 3 days (membrane cut-off 3.5 kDa) followed by lyophilization. Rhodamine-azide was synthetized as reported in other works.[19] The final click reaction was performed between propargyl alginate and rhodamine-azide, exploiting the CuAAC reaction. Summarizing, propargyl alginate (125 mg, 1 eq.) was dissolved in 15 ml of distilled water, while rhodamine-azide (100 mg, 0.6 eq.) in 4 ml of distilled water in a different flask. Once dissolution is complete, the rhodamine containing solution was added dropwise to the alginate containing one. At this point, catalytic amount of copper iodide and sodium ascorbate was added to the reacting mixture, and the reaction was kept at 60 °C for 24 h in a dark environment. Purification step involved dialysis for 3 days (membrane cut-off 3.5 kDa) followed by lyophilization. The successful functionalization of sodium alginate was confirmed by FT-IR analysis (Fig. S1 in the supplementary material). For the experiments, fluorescently labeled sodium alginate was mixed with unlabeled 3% (w/v) sodium alginate aqueous solution at a volume ratio of 1:10 and used for subsequent experiments. Note that 3% was the maximum concentration suitable for filter sterilization due to the high viscosity of the alginate solutions.

### C. Preparation of collagen-alginate mixed pre-gel solution

Collagen pre-gel solution was prepared as the manufacturer's protocol. Briefly, to prepare the buffer for collagen reconstitution, 10 mM $NaHCO_3$ aq. was prepared. Then, 10 mM $NaHCO_3$ aq. and 10 mM 4-(2-hydroxyethyl)-1-piperazineethanesulfonic acid (HEPES) (ThermoFisher) were mixed. The collagen pre-gel solution was reconstituted by mixing the reconstitution buffer, 10× Hank's equilibrium salt solution (Sigma-Aldrich), and various collagen solutions (KOKEN) in a 1:1:8 volume ratio. The reconstituted collagen precursor solutions were maintained at 4 °C on crushed ice.

To prepare the sodium alginate solution, sodium alginate (Wako) was dissolved in de-ionized water (DI water) which was produced by the Millipore purification system. When we use fluorescently labeled alginate, sodium alginate was chemically modified with rhodamine.

Mixed pre-gel solutions were prepared by mixing reconstituted 4 mg/ml collagen precursor solution [stained with NHS-Alexa 488 (ThermoFisher)] and 3% (w/v) sodium alginate solution (chemically modified) in 100:0, 80:20, 60:40, 50:50, 40:60, 20:80, and 0:100 volume ratios.

### D. Fabrication of collagen microgel beads

The mixed pre-gel solution was filled into a syringe fitted with a glass tube tapered to 230 $\mu$m at the tip. The mixed pre-gel solution dropped into 40 mM calcium chloride solution in a 100 mm dish to form calcium alginate microgel beads containing collagen pre-gel solution. Then after that, we quickly replaced the calcium chloride solution with culture medium (DMEM supplemented with FBS and PS). To gelatinize collagen completely, the microgel beads were incubated at 37 °C in an incubator for 3 h. Then, 40 $\mu$l of alginate lyase (40 $\mu$g/ml) (Sigma-Aldrich) was added to the medium to decompose the calcium alginate hydrogel network in the microgel beads. The microgel beads were again placed in the incubator at 37 °C for 1 h. Then after that, the medium in the dish was removed and new culture medium was added.

### E. Observation setup

An inverted fluorescent microscope (Olympus, IX73P1-22FL/PH) with a charge-coupled-device camera (DP73 and cellSens Imaging Software) and a confocal microscope (Olympus, FV3000) with a charge-coupled-device camera (Fluoview, FV31S-SW) were used to observe the microbeads.

### F. Fluorescence intensity analyses on fluorescently labeled alginate and collagen hydrogels

The fluorescence intensity of fluorescently labeled alginate and collagen gel was analyzed using ImageJ every 10 min after the addition of alginate lyase. The area of the microgel beads was determined by the phase contrast image. The determined areas of the microgel beads were superimposed on the fluorescence image using "ROI manager." Then, we used "Mean gray value" to calculate average fluorescence intensity of the bead shape portion in the fluorescence image.

### G. Fabrication of coaxial nozzle device

Hollow collagen microgel beads were prepared using a glass coaxial nozzle device or a 3D-printed coaxial nozzle device.

The glass coaxial nozzle device consists of a glass capillary (OD: 1.0 mm, ID: 0.6 mm, G-1, NARISHIGE), a square glass capillary (OD: 1.4 mm, ID: 1.0 mm, 8100-100, VitroCom), and a plastic connector. The round glass capillaries and square glass capillaries were sharpened with a puller (NARISHIGE). The tips of the round glass and square glass capillaries were cut with a microforge (NARISHIGE) to adjust the tip diameter to 50 and 300 $\mu$m, respectively. To reduce the effects of surface tension, the tips of the glass capillaries were treated with Fluorosurf (KYOKUTO SHOKAI) to repel water. The connectors were fabricated using a 3D printer (AGILISTA, Keyence). The glass capillaries and connectors were assembled on a glass slide (Matsunami Glass Industries) and fixed with adhesives.

The 3D-printed device was fabricated using a microArch S230 (BMF). The microchannel for the inner (core) solution was designed to have an inner diameter of 100 $\mu$m, while that for the outer (shell) solution had an inner diameter of 600 $\mu$m. To prevent leaching from the device, the surface was coated with a ~0.3 $\mu$m thick parylene layer. In addition, hydrophobic treatment was applied using a Fluorosurf, as in the case of the glass device.

### H. Fabrication of hollow collagen microgel beads

To prepare hollow collagen microgel beads, two solutions were prepared. (1) Core flow: 10% PBS (–) (Wako) (visualized by red fluorescence beads). (2) Shell flow: A solution of 3.0% (w/v) sodium alginate (Wako) and 4 mg/ml collagen solution (stained with NHS-Alexa 350) mixed at 2:3. The presence of calcium ions in the core solution can initiate alginate gelation during droplet formation. Therefore, a calcium-free solution, such as PBS or saline, is required as the core solution. In this study, PBS was used as the suspension fluid for the cells. The prepared solutions were filled into syringes, connected to the double-coaxial nozzle device using Teflon tubes (Shimadzu). The syringe was set in a laboratory-made syringe pump. The core solution was injected at a flow rate of 20–40 $\mu$l/min and the shell at 160–180 $\mu$l/min in a refrigerator (4 °C). Two solutions were dropped to form microgel beads using the coaxial nozzle device. The throughput of this fabrication process was approximately 30 beads per minute. The microgel beads were collected in 25 ml tube containing 100 mM calcium chloride solution with 2.8% surfactant (Tween20, Tokyo Chemical Industry). The critical micelle concentration (CMC) of Tween 20 has been reported to be 0.0342 mM at 40 °C, which is close to the experimental temperature of 37 °C. It is expected that the CMC would be slightly lower in the presence of $CaCl_2$ aq.[20,21] The distance between the device tip and the surface of the calcium ion solution was set to 15 mm at that time. Then, we promptly replaced calcium chloride solution with medium. To gelatinize collagen completely, the microgel beads was incubated at 37 °C for 3 h. Then, 20 $\mu$l of alginate lyase (40 $\mu$g/ml) was added for the bead with 1 ml of medium to degrade the calcium alginate gel. To revitalize alginate lyase, microbeads were again incubated at 37 °C for 1 h. After that, microgel beads were washed with medium.

### I. Fabrication of NIH/3T3 cell-encapsulating hollow collagen microgel beads

To prepare NIH/3T3 cell-encapsulating hollow collagen microgel beads, two solutions were prepared. (1) Core flow: NIH/3T3 cells were suspended in PBS at a concentration of $1.0 \times 10^7$ cells/ml to prepare cell suspension. (2) Shell flow: A solution of 3.0% (w/v) sodium alginate (Wako) with 0.88% (w/v) NaCl aq. and 4 mg/ml collagen solution mixed at 2:3. Fabrication setup was same as for collagen microgel beads. The core solution was injected at a flow rate of 10 $\mu$l/min and the shell at 190 $\mu$l/min. The microgel beads were collected in 25 ml tube containing 40–100 mM calcium chloride solution with 0.0%–3.0% surfactant. To match the osmolarity of the solution with the intracellular osmolarity (~300 mOsm/l), NaCl was added to 40 mM $CaCl_2$ to a final concentration of 0.56% (w/v). Then, we promptly replaced calcium chloride solution. with 145 mM NaCl aq., followed by replacement with the medium (DMEM with FBS and PS). Using the same procedure as hollow collagen microgel beads, cell-encapsulating hollow collagen microgel beads were obtained.

### J. Investigation of surfactant concentration

To investigate the concentration of surfactant added to the calcium chloride solution, hollow collagen microgel beads were fabricated under five different conditions (Surfactant concentration = 0%, 0.05%, 0.1%, 1.0%, and 3.0%). The core and shell solutions were prepared following the same procedure as that used for the fabrication of hollow collagen microgel beads. The prepared solutions were filled into syringes, connected to the 3D-printed coaxial nozzle device. The syringe was set in a laboratory-made syringe pump. The core solution was injected at a flow rate of 10 $\mu$l/min and the shell at 190 $\mu$l/min in a refrigerator (4 °C). Two solutions were dropped to form microgel beads using the 3D-printed coaxial nozzle device. The microgel beads were collected in 25 ml tube containing 100 mM calcium chloride solution with surfactant. The distance between the device tip and the surface of the calcium ion solution was set to 15 mm at that time. Then, we promptly replaced calcium chloride solution with 145 mM NaCl aq., followed by replacement with DMEM. Using the same procedure as hollow collagen microgel beads, hollow collagen microgel beads were obtained.

### K. Fabrication of HUVEC-encapsulating hollow collagen microgel beads

To prepare HUVEC-encapsulating hollow collagen microgel beads, two solutions were prepared. (1) Core flow: HUVECs (P6) were suspended in PBS at a concentration of $1.0 \times 10^7$ cells/ml to prepare cell suspension. (2) Shell flow: A solution of 3.0% (w/v) sodium alginate (Wako) with 0.88% (w/v) NaCl aq. and 4 mg/ml collagen solution mixed at 2:3. Collagen was stained with NHS-Alexa 350 (ThermoFisher). Fabrication setup was same as collagen microgel beads. The core solution was injected at a flow rate of 10 $\mu$l/min and the shell at 190 $\mu$l/min. The microgel beads were collected in 25 ml tube containing 100 mM calcium chloride solution with 0.05% surfactant. Then, we promptly replaced calcium chloride solution with 145 mM NaCl aq., followed by replacement with the medium (Endothelial Basal Medium with FBS). Using the same procedure as hollow collagen microgel beads, cell-encapsulating hollow collagen microgel beads were obtained. After that, microbeads were cultured in medium at 37 °C in a 5% $CO_2$ atmosphere for 7 days.

### L. Viability assay

To investigate the viability of the encapsulated cells in the encapsulation process, 2 $\mu$M calcein AM (Wako) and 4 $\mu$M EthD-1 (Wako) were added to the medium containing the microbeads encapsulating cells. The medium was then incubated at 37 °C for 10 min to react to the live/dead assay reagents. After incubation, the microgel beads were washed with PBS. Survival rates were calculated by measuring the areas of live and dead cells in three images per bead taken at different focal points using "Analyze particle" of ImageJ.

### M. Fluorescent immunostaining

To observe signals of DAPI and CD31, the hollow collagen microgel beads were fixed with 4% paraformaldehyde phosphate buffer solution (Wako). Furthermore, the hollow collagen microgel beads were permeabilized with 0.2% Triton X-100 (Sigma) in PBS (–). After blocking treatment with 5% bovine serum albumin (BSA, Sigma-Aldrich) in PBS (–), the hollow collagen microgel beads were incubated with primary antibodies against CD31 produced in mouse (1:400; Bio-Techne Japan) at 4 °C overnight. After rinsing, the hollow collagen microgel beads were incubated with anti-mouse IgG-Alexa Fluor 568 (1:200; Invitrogen) and the treatment of DAPI [1 $\mu$g/ml in PBS (–), Invitrogen] for nucleus staining. After fluorescent staining, the microgel beads were observed by a confocal microscope. Images were captured at 40× magnification using a 10× lens and 4× digital zoom.

## III. RESULTS AND DISCUSSION

### A. Fabrication and evaluation of hollow collagen microgel beads

#### *1. Principle of fabricating cell-encapsulating collagen hollow microgel beads*

The collagen hollow microgel beads proposed in this study are fabricated using an alginate template method based on the previous work.[22] Calcium alginate gel serve as a molecular template, allowing rapid formation of beads via instantaneous gelation of sodium alginate with calcium ions. Two solutions were prepared: (i) a mixed pre-gel solution of sodium alginate (3 w/v%) and collagen (4 mg/ml) for the shell and (ii) PBS containing cells for the core. Both solutions were dispensed into a calcium chloride solution (40–100 mM) through a coaxial nozzle device (Fig. S2 in the supplementary material).[15] Surfactant (Tween 20, 0.05%–3%) was added to calcium chloride solution to minimize the impact at the liquid surface.[23] Sodium alginate was instantly crosslinked by calcium ions, forming the core–shell beads. Collagen within the alginate network was subsequently solidified by incubation at 37 °C. After full collagen gelation, the alginate gel was selectively degraded by alginate lyase (final concentration: 77 $\mu$g/ml) resulting in shells primarily composed of

collagen, a tissue-derived ECM. Encapsulated cells in the core adhered to the inner collagen wall, facilitating the formation of a hollow tissue structure within the beads (Fig. 2).

This method is straightforward and enables mass production of uniform microgel beads in a single batch. To optimize the conditions of the bead fabrication, the appropriate mixing ratios of collagen and alginate gel were evaluated. Furthermore, the efficiency of alginate gel degradation by alginate lyase and the effect of surfactant concentration on bead morphology and cell viability were systematically investigated.

### 2. Fabrication and evaluation of hollow collagen microgel beads

To determine the optimal mixing ratio of collagen and alginate, collagen microgel beads were fabricated using seven different mixing ratios of alginate to collagen (100:0, 80:20, 60:40, 50:50, 40:60, 20:80, and 0:100). The resulting microgel beads were evaluated for their morphological characteristics, specifically the roundness, using top and side view images [Fig. 3(a) and Table I].

The roundness value of the collagen microgel beads fabricated at sodium alginate to collagen volume ratios of 60:40, 50:50, and 40:60 were all 0.90 or higher, indicating that the beads were essentially as spherical. In contrast, microgel beads prepared with the 20:80 ratio exhibited a roundness of 0.76, suggesting an elliptical morphology. For the 100:0 ratio, the beads were completely dissolved by alginate lyase treatment. Bead formation was unsuccessful at both 80:20 and 0:100 ratios. The elliptical shape observed at the 20:80 ratio suggests that the amount of alginate was insufficient to maintain a spherical structure during fabrication. At ratio of 80:20 and 0:100, the beads collapsed after degradation of alginate gel. These findings demonstrate that sodium alginate to collagen ratios of 60:40, 50:50, and 40:60 are optimal for producing stable, spherical microgel beads using our method. Among these, we adopt the 40:60 ratio for subsequent experiments, as it provides the highest collagen content (Fig. S3 in the supplementary material).

### 3. Degradation of alginate gel

To verify the selective degradation of alginate gel by alginate lyase, fluorescent measurement was conducted using fluorescently labeled alginate and collagen. The changes in fluorescence intensities of the alginate gel and collagen gel for 1 h after the addition of alginate lyase were evaluated [Figs. 3(b) and S3 in the supplementary material] ($n = 4$, mean ± s.d.). Specifically, the averaged fluorescence intensities of both alginate and collagen were quantified at 10 min interval post-treatment. As a control, the beads without alginate lyase treatment were also evaluated [Fig. 3(c)]. The result shows that, in the absence of alginate lyase, the normalized fluorescence intensities of the collagen gel ($I_{collagen}$) and the alginate gel ($I_{alginate}$) remained relatively unchanged over 60 min [$I_{collagen}$ at 60 min = 1.02 ± 0.011 55 (mean ± s.d., $I_{alginate} = 0.96$ at 60 min)]. In contrast, upon treatment

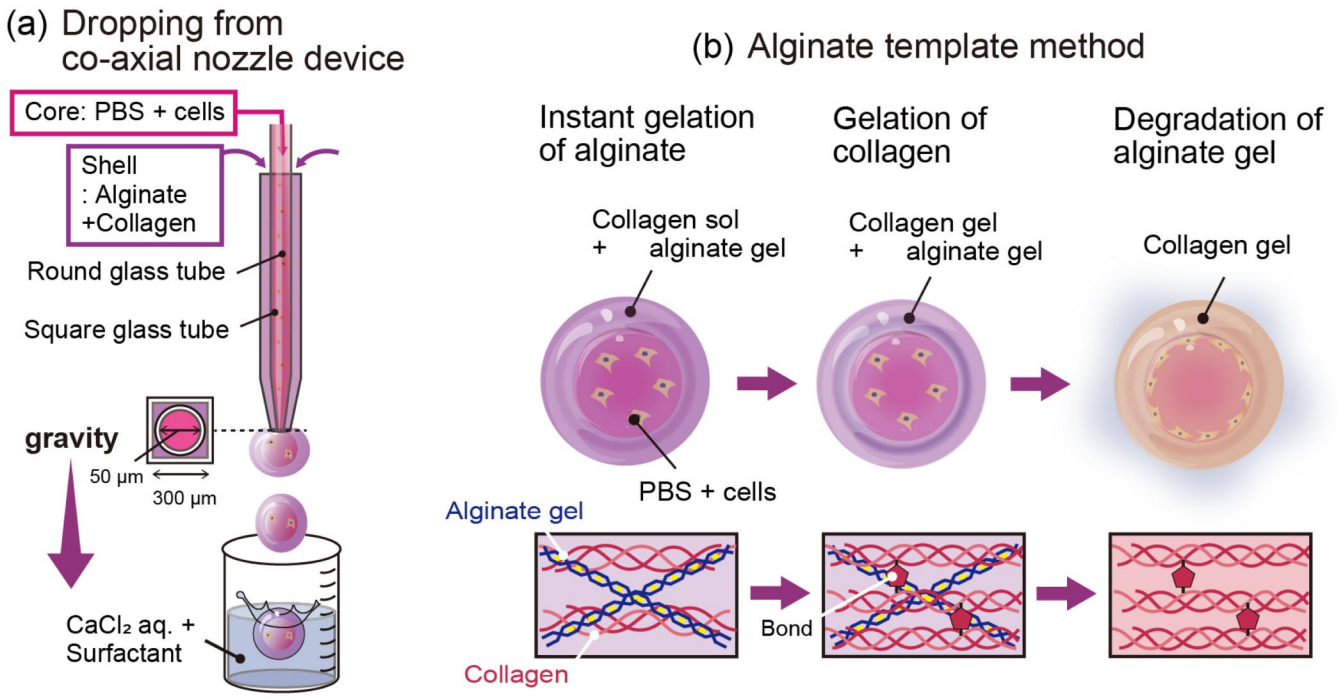


**FIG. 2.** Fabrication of our cell-encapsulating hollow collagen microgel beads. (a) As a first step, double-layered droplets are dropped from a coaxial nozzle device. (b) As a second step, the alginate template method is used to form beads primarily composed of collagen.

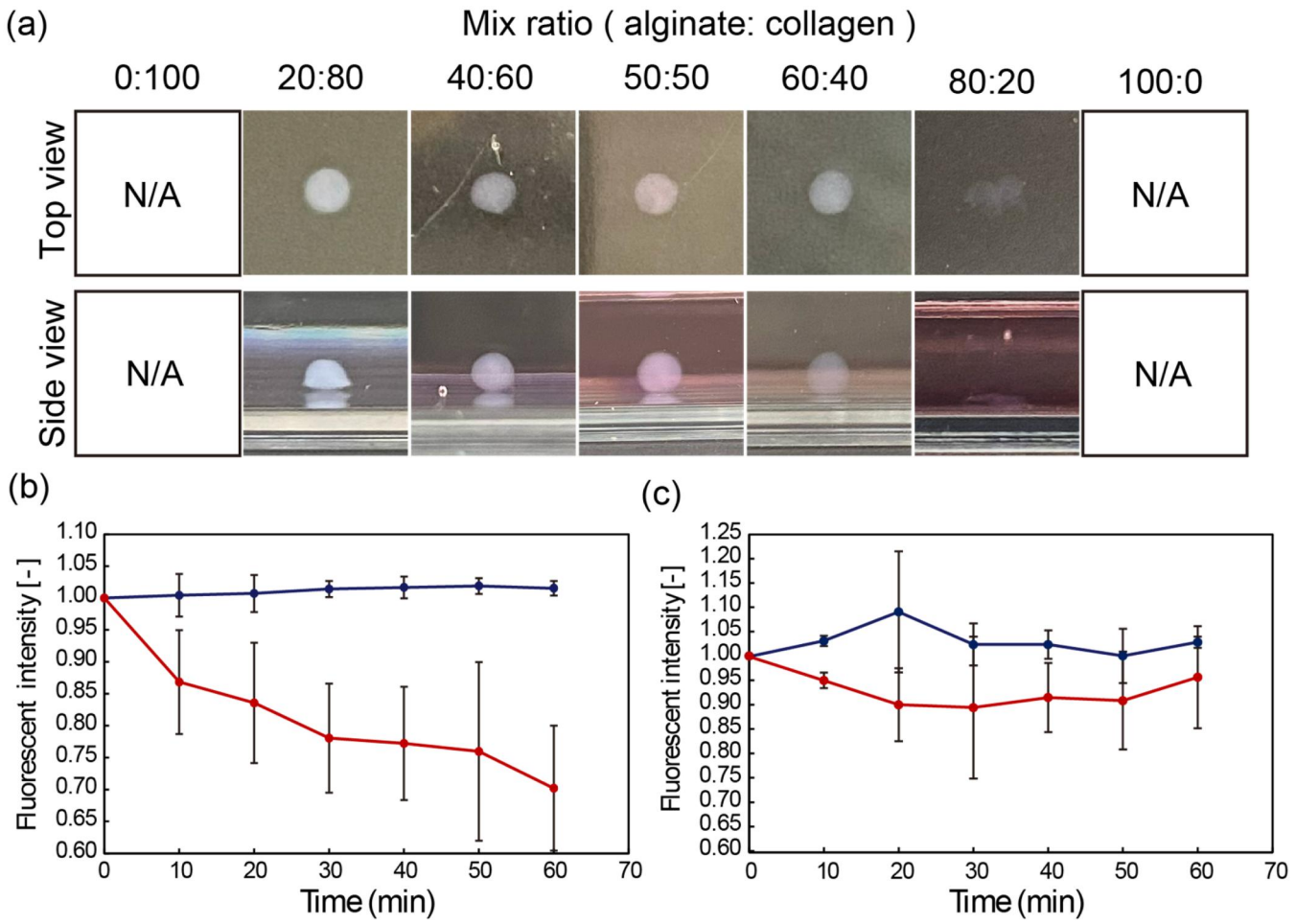


**FIG. 3.** Evaluation of the fabrication method of collagen microgel beads. (a) Images of fabricated collagen microgel beads with different mixing ratios of sodium alginate and collagen. (b) Time-lapse fluorescent measurement of alginate (red) and collagen (blue) with alginate lyase treatment ($n = 4$, mean ± s.d.). (c) Time-lapse fluorescent measurement of alginate (red) and collagen (blue) without alginate lyase treatment ($n = 4$, mean ± s.d.).

with alginate lyase, the fluorescence intensity of the alginate gel decreased significantly ($I_{alginate} = 0.70$ at 60 min), while the collagen gel was unaffected. These results confirm that alginate lyase selectively degrades the alginate gel, leaving the collagen gel intact.

### 4. Regulation of core size in collagen microgel beads

To investigate the control of core size by the flow ratio of core to shell, hollow collagen microgel beads were prepared at three different flow ratios [shell ($\mu$l/min): core ($\mu$l/min) = 160:40, 170:30, and 180:20], keeping the total flow-rate constant at 200 $\mu$l/min (Fig. S4 in the supplementary material). The shell solution consisted of a mixed pre-gel of sodium alginate and collagen, while the core contained PBS. These solutions were dispensed into calcium chloride solution (100 mM) with 2.8% surfactant through the coaxial nozzle device. Finally, the alginate gel was selectively decomposed by alginate lyase to obtain collagen hollow microgel beads as described in Sec. D.

**TABLE I.** Evaluation of the shape of the collagen microgel beads with different mixing ratios of sodium alginate and collagen.

| Mix ratio (%) (3% sodium alginate : 4 mg/ml collagen) | 0:100 | 20:80 | 40:60 | 50:50 | 60:40 | 80:20 | 100:0 |
|---|---|---|---|---|---|---|---|
| Averaged roundness ($n = 5$) | n/a | 0.7620 | 0.9256 | 0.9426 | 0.9259 | n/a | n/a |
| Standard deviation | n/a | 0.055 02 | 0.026 18 | 0.016 16 | 0.040 52 | n/a | n/a |

The core and shell diameters of the fabricated hollow collagen microgel beads were measured from fluorescence images. The results demonstrated that increasing the flow rate of the core relative to the total flow rate resulted in larger core sizes and thinner shell thickness [Figs. 4(a), 4(b) and 4(c)], indicating that the core size can be controlled by adjusting the flow ratio. In addition, no significant differences in bead circularity were observed across the flow-rate conditions [Fig. 4(d)]. The diameter distribution of the fabricated hollow collagen microgel beads [shell:core = 180:20 ($\mu$l/min)] were analyzed [Fig. 4(e)], yielding the average core and shell diameters of

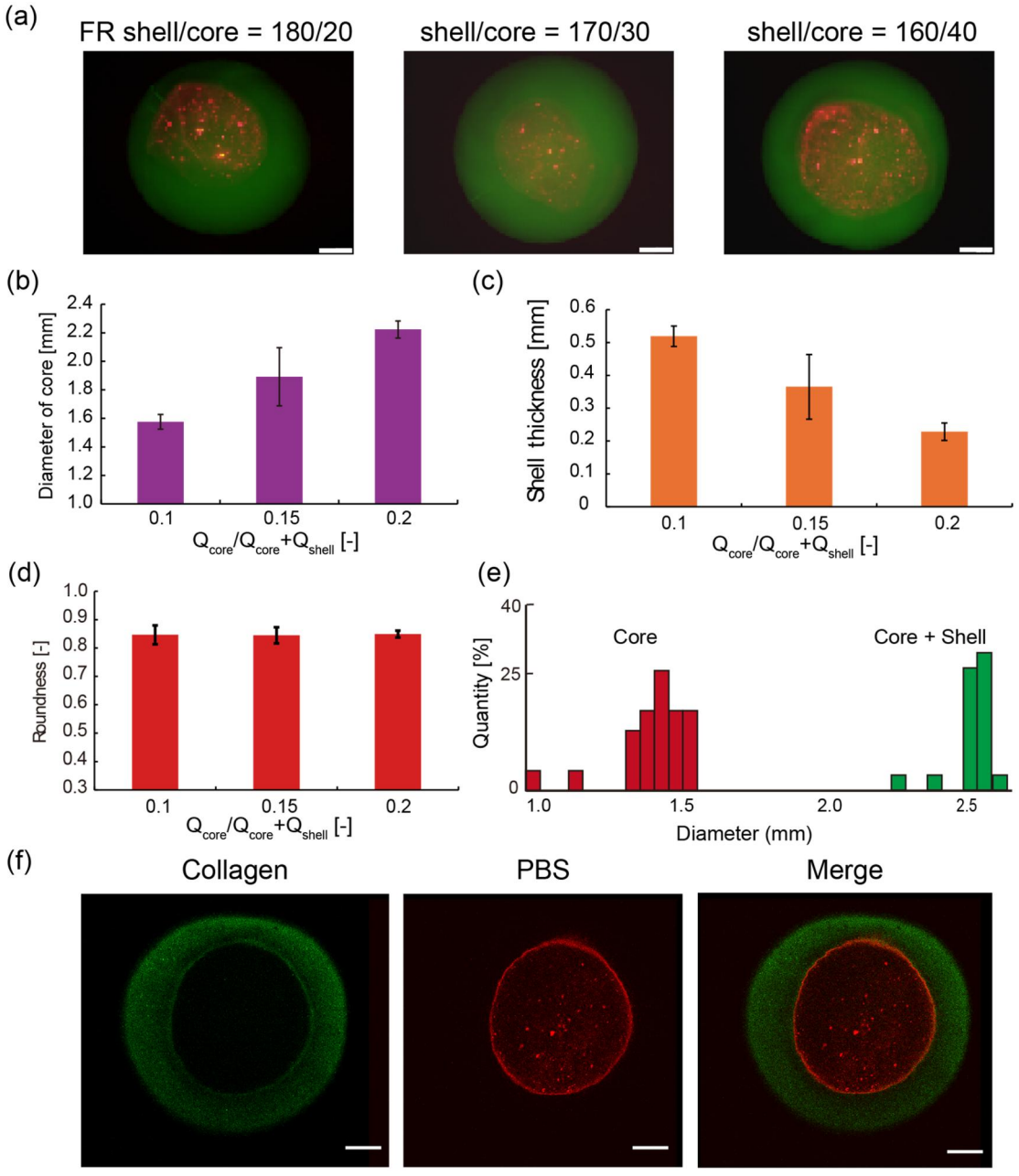


**FIG. 4.** Evaluation of the fabricated hollow collagen microgel beads. (a) Fabricated hollow collagen microgel beads with different flow rate (FR) of core and shell stream. (b) Core diameter at three different flow ratios. (c) Shell thickness at three different flow ratios. (d) Bead roundness at three different flow ratios. (e) Distribution of the diameter of core (red) and shell (green) ($n = 23$). (f) Slice image of fabricated hollow collagen microgel beads (green: collagen and red: PBS).

1.4 ± 0.13 and 2.5 ± 0.07 mm (mean ± s.d.), respectively. The corresponding coefficients of variation (CVs) were 9.4% for the core and 2.8% for the shell. Confocal microscopy further confirmed the successful fabrication of hollow-structured collagen microgel beads [Fig. 4(f); shell:core = 160:40 ($\mu$l/min)].

### 5. Effect of surfactant on the shape and cell viability of the hollow collagen microgel beads

In the process of encapsulating cells in the hollow collagen microgel beads, concentration of calcium chloride solution and surfactant are expected to affect cell viability. To evaluate these effects, NIH/3T3 cell-encapsulating hollow collagen microgel beads were prepared under four different conditions [40 or 100 mM calcium chloride solution and 0% or 3.0% surfactant; Fig. 5(a)]. Immediately after the fabrication, cell viability was evaluated. The results indicated that cell viability was highest at a surfactant concentration of 0%, whereas most cells died at 3.0% surfactant. The concentration of the calcium chloride solution did not significantly affect the cell viability. Notably, the roundness of the beads was quantified as 0.595 (40 mM $CaCl_2$ aq., 0% surfactant), 0.735 (100 mM $CaCl_2$ aq., 0% surfactant), 0.947 (40 mM $CaCl_2$ aq., 3.0% surfactant), and 0.869 (100 mM $CaCl_2$ aq., 3.0% surfactant). These results indicate that the beads formed without

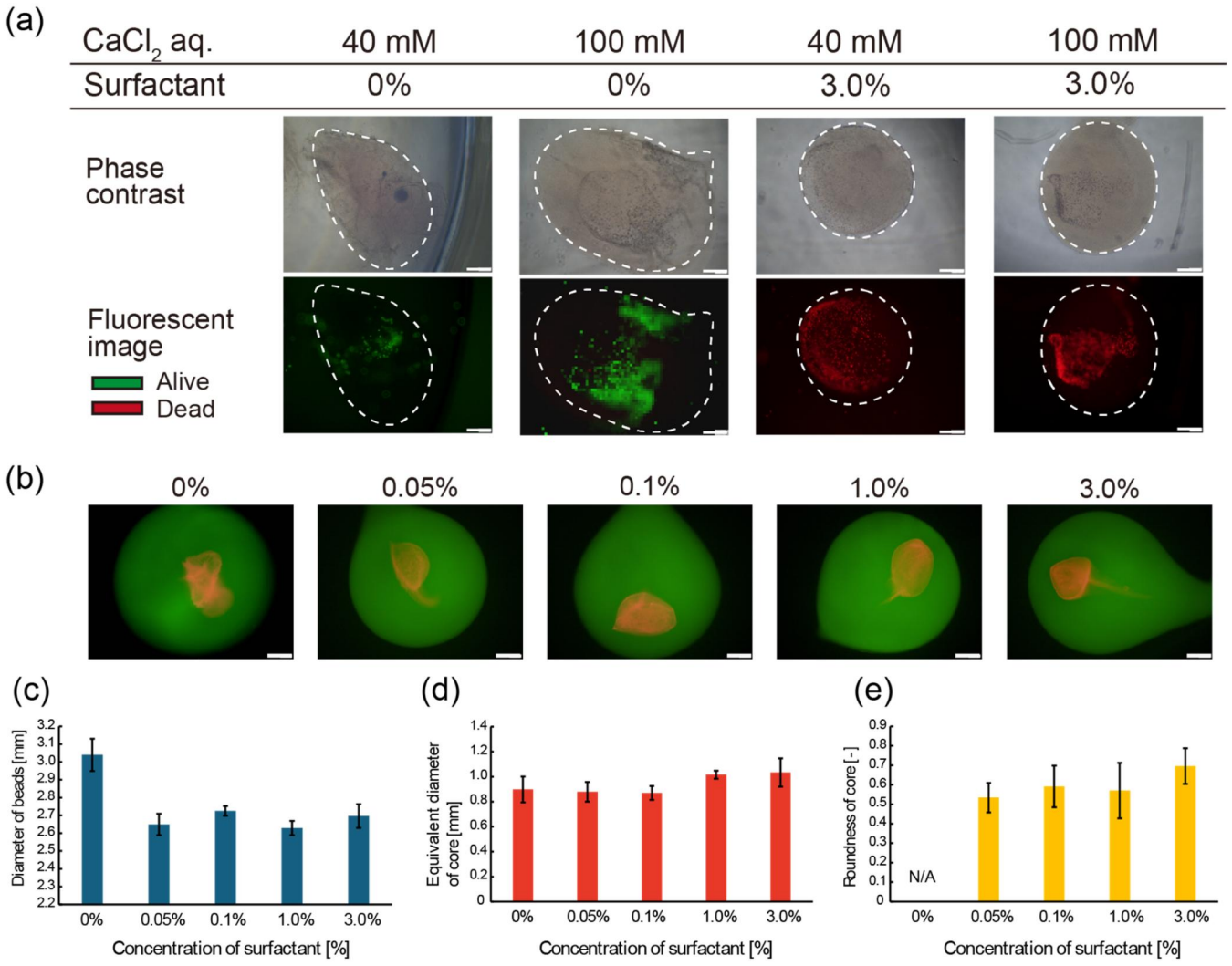


**FIG. 5.** Evaluation of the concentration of surfactant and $CaCl_2$ aq. (a) Fabricated NIH/3T3 cell-encapsulating hollow collagen microgel beads with different concentrations of surfactant and calcium chloride solution. Scale bars for the images are 400 $\mu$m. (b) Fabricated hollow collagen microgel beads under five different concentrations of surfactant. Scale bars for the images are 400 $\mu$m. (c) Bead diameter at five different concentrations ($n$ = 5, mean ± s.d.). (d) Equivalent core diameter at five different concentrations ($n$ = 5, mean ± s.d.). (e) Core roundness at five different concentrations ($n$ = 5, mean ± s.d.).

surfactant (0%) exhibited an irregular shape, while those formed at 3.0% surfactant were more spherical. In addition, no substantial differences in bead morphology were observed between the different calcium chloride concentrations. This is likely because sodium alginate undergoes rapid ionic cross-linking, forming a gel within milliseconds under both conditions.

These findings highlight that the surfactant concentration strongly affects cell viability and bead morphology. To investigate the effect of surfactant concentration on bead morphology, hollow collagen microgel beads were prepared under five different surfactant concentrations (0%, 0.05%, 0.1%, 1.0%, and 3.0%) [Fig. 5(a)]. The resulting bead morphology showed that, at 0%, the beads exhibited a slightly flattened, non-spherical shape, whereas under all other conditions, the beads were nearly spherical. Based on the fluorescence images, the overall bead diameter, core diameter, and core roundness were quantified [Figs. 5(c), 5(d) and 5(e)]. The overall bead diameter was found to be larger only at 0% compared to the other conditions, which is likely due to the deformation and spreading of the beads. In addition, as observed in the fluorescence images, the core structure at 0% was distorted. Therefore, roundness was compared among the conditions excluding 0%, and no significant differences were observed. These results indicate that bead morphology was not substantially affected within the range of 0.05%–3.0%. Considering the minimal impact on cell viability, a concentration of 0.05% was selected for subsequent experiments (Fig. S6 in the supplementary material).

## B. Encapsulation of HUVECs in hollow collagen microgel beads

### 1. Fabrication of HUVEC-encapsulating hollow collagen microgel beads

To evaluate whether HUVECs can be effectively encapsulated and cultured within hollow collagen microgel beads, we conducted encapsulation and subsequent culture experiments. HUVECs were suspended in PBS at a concentration of $1.0 \times 10^7$ cells/ml for the core solution. A high cell concentration was used to account for cell sedimentation within the syringe. The hollow collagen microbeads were as described in Secs. 2 and 3 with flow rates set to 10 $\mu$l/min and shell was set at 190 $\mu$l/min. Immediately after the beads formation, the beads were incubated in culture medium on a shaking incubator for 3 h to uneven cell distribution. Following incubation, the alginate hydrogel network was degraded via alginate lyase treatment. Observation with a phase contrast microscope confirmed that the HUVECs were encapsulated inside the beads [Fig. 6(a)]. The beads were then cultured for 7 days. During this period, the cells were observed to adhere to the inner wall and cover the surface of the hollow collagen beads.

### 2. Viability of HUVECs in the hollow collagen microgel beads

To evaluate whether HUVECs remained viable within the beads and was capable of forming tissue, a viability assay was performed, and cell viability was assessed using a qualitative image-based analysis. Immediately after the bead preparation, 2 $\mu$M calcein AM and 2 $\mu$M EthD-1 were added to the medium containing the microgel beads, and a fluorescence microscopy was used for observation. The initial viability of the encapsulated HUVECs was estimated to be 83%. After 6 days of culture, the estimated cell viability increased to 90%, indicating that the cells can remained viable inside the beads over an extended period, likely due to adequate the exchange of nutrients and waste products [Figs. 6(b) and S7(a) in the supplementary material]. These results demonstrate that HUVECs can be maintained at high viability within the fabricated hollow collagen microgel beads. Additionally, five beads were randomly selected each day from those under culture, and their size and roundness were measured [Figs. 6(c) and 6(d)]. The results showed no significant change in roundness; however, the bead size gradually decreased over time. This suggests that the cells within the beads adhered to the surrounding matrix and exerted contractile forces, pulling the matrix inward.

### 3. Confocal microscopic observation of hollow collagen microgel beads

To confirm the tissue formation by HUVECs, confocal microscopy was employed. Collagen gel was visualized by NHS-Alexa 350, and the HUVECs were visualized by calcein AM and EthD-1. Confocal image on day 2 shows that cells adhered to the inner collagen wall, forming a hollow tissue structure [Fig. 6(e)]. In addition, fluorescent immunostaining was performed on the beads using antibodies against CD31, endothelial cell marker. The presence of CD31 (red) confirmed the endothelial phenotype of HUVECs [Figs. 6(f) and S7(b) in the supplementary material].[24] This image also confirmed that the cells formed a hollow structure. This observation confirmed that HUVECs form a hollow tissue structure within the collagen microgel beads.

## C. Discussion

In this study, we successfully formed hollow-shaped HUVEC tissues using hollow collagen microgel beads. A key innovation of our approach is that stable fabrication of hollow tissues is achieved without relying on self-organization ability of cells, which is typically required for *in vitro* tissue formation. Although the formation of hollow tissues within microgel spheres has been reported previously,[25,26] these constructs generally possess solid inner layer or they only exhibit a cell-to-cell adhesion. In contrast, a key characteristic of hollow tissues in humans is that their inner cavities are lined with endothelial cells adhering to the outer ECM, while their interiors are hollow cavities with solutions.[27–29] From this perspective, our method provides a unique platform to engineer such physiologically relevant hollow tissue structures.

Notable outcomes of our study include (i) the successful fabrication of a liquid-filled hollow structure lined with endothelial cells, (ii) high viability of encapsulated HUVECs, with approximately 90% survival on the inner surface of the hollow microgel beads after one week of culture, and (iii) confirmed CD31 expression, indicating the maintenance of endothelial phenotype and tissue-specific structural functions. Together, these results demonstrate that hollow collagen microgel beads are effective scaffolds for the formation of hollow tissues *in vitro*. We anticipate that this technique can be applied to the engineering of various hollow organ-like tissues, such as heart models.

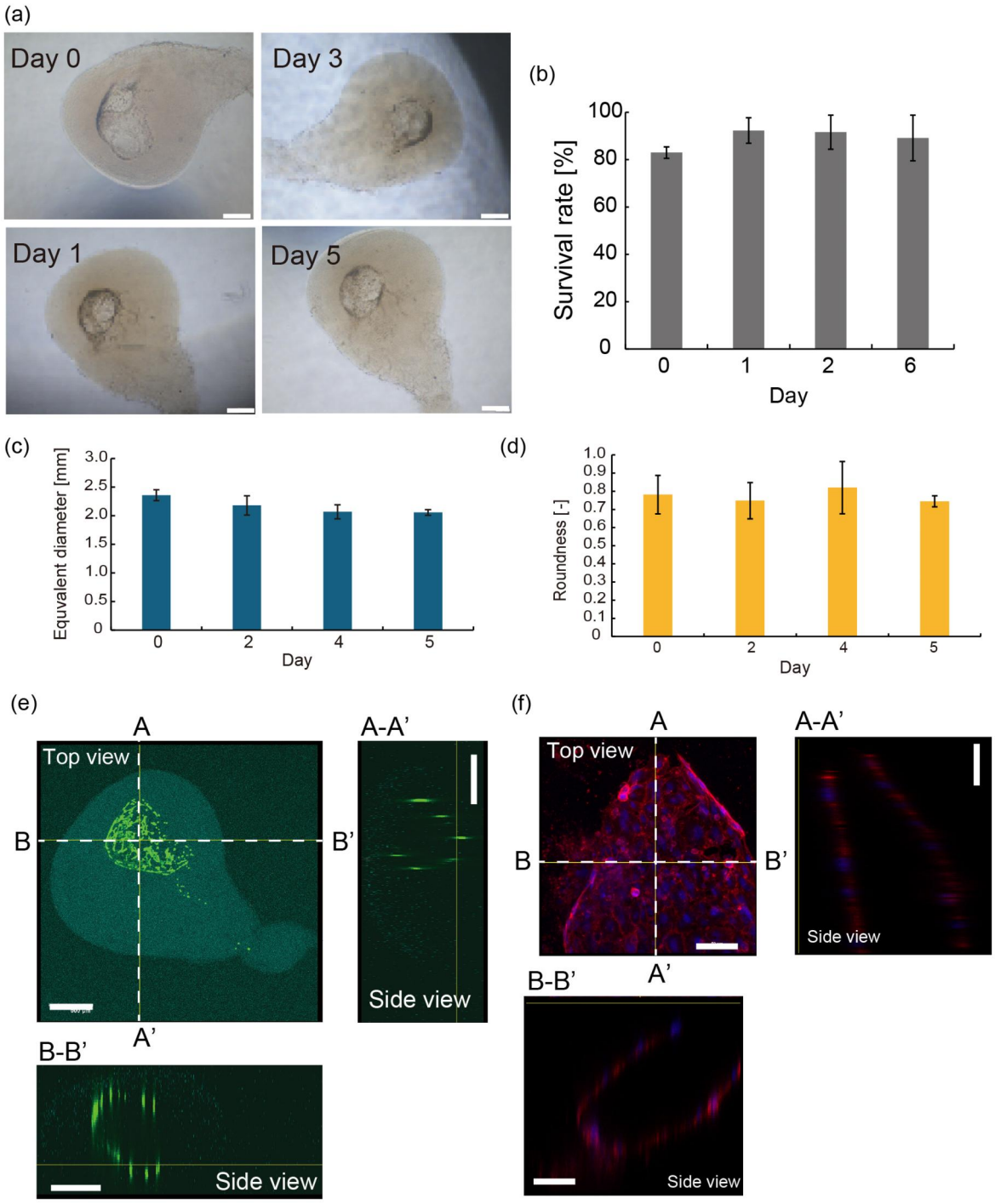


**FIG. 6.** Fabricated HUVEC-encapsulating hollow collagen microgel beads. (a) Cultivation of the HUVEC-encapsulating hollow collagen microgel beads on day 0, 1, 3, and 5. (b) Survival rate of HUVECs encapsulating in the hollow collagen microgel beads ($n = 3$, mean ± s.d.). (c) Equivalent diameter of the HUVEC-encapsulating hollow collagen microgel beads on day 0, 2, 4, and 5 ($n = 5$, mean ± s.d.). (d) Roundness of the HUVEC-encapsulating hollow collagen microgel beads on day 0, 2, 4, and 5 ($n = 5$, mean ± s.d.). (e) Confocal microscopic image of the HUVEC-encapsulating hollow collagen microgel beads on day 2 (green and red: HUVECs and blue: collagen gel). (f) Confocal microscopic image of the immunostaining of the HUVEC-encapsulating hollow collagen microgel beads on day 2 (blue: DAPI and red: CD31).

One of the major remaining challenges is the non-uniformity of bead shape. In particular, the roundness of the HUVEC-encapsulating hollow collagen microgel beads prepared in this study was 0.66 ($n = 5$, day 5), indicating a deviation from an ideal spherical geometry. This deformation is likely attributable to the presence of encapsulated cells, which causes the fluid to behave as a particle-laden flow, thereby disturbing the flow profile. To address this issue, increasing the viscosity of the core solution may be an effective strategy to suppress such flow disturbances. In addition, factors other than those examined in this study—such as the dropping height, the geometry of the device, and the diameter of the device tip—are also expected to significantly influence bead morphology. Therefore, optimization of these parameters will be necessary to improve the uniformity and sphericity of the beads.

In addition, the wall integrity and degradation of the collagen gel are important factors for long-term culture. In our experiment, no remarkable degradation or collapse of the collagen shell have been observed in 7-day culture. Previous studies have also reported successful culture periods exceeding 30 days, suggesting that these materials possess sufficient stability under such conditions.[30] On the contrary, physical characteristics of scaffolds have known to be a critical parameter in tissue formation and differentiation. Thus, precise analyses on the changes of the mechanical property could give us an effective information to design these hollow beads for further tissue formation and maturation.

One of the key characteristics of endothelial cells is their ability to form tube-like, vessel-like structures. Future studies evaluating such functional properties will provide more comprehensive evidence that the proposed microgel beads can operate as functional tissue constructs. Indeed, previous studies have demonstrated that endothelial cells are capable of forming tube-like vascular structures within *in vitro* tissues composed of similar collagen-based matrices.[31]

We believe that this technology can be extended to the formation of artificial heart organoids. By encapsulating cardiomyocytes and fibroblasts in the shell and endothelial cells in the core of the hollow collagen microgel beads, it may be possible to recapitulate the tissue architecture of an early stage developing heart. Recent advances in heart organoid research have enabled the modeling of cardiac diseases.[32,33] For example, gene knockout techniques combined with heart organoids have been used to model congenital heart disease.[34,35] However, it has been observed that knockout of developmentally important genes can prevent organoid self-organization and cardiac structure formation. Furthermore, the success rate of heart organoid formation is influenced by both environmental and biological factors.[36] Our approach, which employs an engineered hollow collagen scaffold, enables robust and reproducible formation of hollow tissues, independent of intrinsic cellular self-organization. Such engineered heart organoids could serve as models for elucidating the pathophysiology of congenital heart disease and for drug development.

## IV. CONCLUSIONS

In this study, we presented a method for fabricating cell-encapsulating hollow collagen microgel beads using an alginate template approach. Confocal imaging confirmed the successful formation of the hollow structure within the beads. Furthermore, HUVECs were encapsulated into the core of the beads and cultured for seven days. The results demonstrated that HUVECs adhere to the inner surface of the collagen shell and maintained their viability and function within the beads. These findings suggest that hollow collagen microgel beads provide a promising platform for *in vitro* models of hollow tissues, which could be valuable for disease modeling and drug evaluation.

## SUPPLEMENTARY MATERIAL

The supplementary material includes FT-IR characterization of modified alginate (Fig. S1), images of the coaxial nozzle devices used for bead fabrication (Fig. S2), evaluation of cell adhesion on collagen beads (Fig. S3), time-lapse fluorescence images after alginate lyase treatment (Fig. S4), images of fabricated hollow collagen microgel beads (Fig. S5), cell survival at different surfactant concentrations (Fig. S6), and confocal observations of HUVECs encapsulated within hollow collagen microgel beads (Fig. S7).

## ACKNOWLEDGMENTS

This work was partly supported by Grant-in-aid for Scientific Research (A) (No. 23H00555), Japan Society for the Promotion of Science (JSPS), Japan.

## AUTHOR DECLARATIONS

### Conflict of Interest

The authors have no conflicts to disclose.

### Ethics Approval

Ethics approval was not required because this study did not involve human participants, animals, or identifiable personal data.

### Author Contributions

**Satona Abeta:** Conceptualization (equal); Investigation (equal); Methodology (equal); Writing – original draft (lead); Writing – review & editing (lead). **Aiki Hioki:** Investigation (supporting); Methodology (supporting). **Akari Masuda:** Investigation (supporting); Methodology (supporting). **Fabio Pizzeti:** Methodology (supporting). **Filippo Rossi:** Methodology (supporting). **Kayoko Hirayama-Shoji:** Conceptualization (equal); Investigation (supporting); Writing – review & editing (supporting). **Hiroaki Onoe:** Conceptualization (equal); Investigation (supporting); Writing – review & editing (supporting).

## DATA AVAILABILITY

The data that support the findings of this study are available from the corresponding author upon reasonable request.

## REFERENCES

[1]Z. Zhao, X. Chen, A. M. Dowbaj, A. Sljukic, K. Bratlie, L. Lin, E. L. S. Fong, G. M. Balachander, Z. Chen, A. Soragni, M. Huch, Y. A. Zeng, Q. Wang, and H. Yu, "Organoids," Nat. Rev. Methods Primers **2**, 94 (2022).
[2]M. Huch and B. K. Koo, "Modeling mouse and human development using organoid cultures," Development **142**, 3113–3125 (2015).

[3]G. Rossi, A. Manfrin, and M. P. Lutolf, "Progress and potential in organoid research," Nat. Rev. Genet. **19**, 671–687 (2018).
[4]H. Xu, X. Lyu, M. Yi, W. Zhao, Y. Song, and K. Wu, "Organoid technology and applications in cancer research," J. Hematol. Oncol. **11**, 1–15 (2018).
[5]A. I. Vazquez-Armendariz and P. R. Tata, "Recent advances in lung organoid development and applications in disease modeling," J. Clin. Invest. **133**, e170500 (2023).
[6]T. Xiang, J. Wang, and H. Li, "Current applications of intestinal organoids: A review," Stem Cell Res. Ther. **15**(1), 155–117 (2024).
[7]L. Li, H. Knutsdottir, K. Hui, M. J. Weiss, J. He, B. Philosophe, A. M. Cameron, C. L. Wolfgang, T. M. Pawlik, G. Ghiaur, A. J. Ewald, E. Mezey, J. S. Bader, and F. M. Selaru, "Human primary liver cancer organoids reveal intratumor and interpatient drug response heterogeneity," JCI Insight **4**, e121490 (2019).
[8]A. O'Connor and C. O'Moráin, "Digestive function of the stomach," Dig. Dis. **32**, 186–191 (2014).
[9]H. Antoni, "Function of the heart," in *Human Physiology* (Springer, 1989), pp. 439–479.
[10]S. Bartfeld and H. Clevers, "Organoids as model for infectious diseases: Culture of human and murine stomach organoids and microinjection of helicobacter pylori," J. Vis. Exp. **2015**, 53359 (2015).
[11]B. Volmert, A. Kiselev, A. Juhong, F. Wang, A. Riggs, A. Kostina, C. O'Hern, P. Muniyandi, A. Wasserman, A. Huang, Y. Lewis-Israeli, V. Panda, S. Bhattacharya, A. Lauver, S. Park, Z. Qiu, C. Zhou, and A. Aguirre, "A patterned human primitive heart organoid model generated by pluripotent stem cell self-organization," Nat. Commun. **14**, 1–22 (2023).
[12]X. Yin, B. E. Mead, H. Safaee, R. Langer, J. M. Karp, and O. Levy, "Stem cell organoid engineering cell," Stem Cell **18**, 25 (2016).
[13]A. Lewis, R. Keshara, Y. H. Kim, and A. Grapin-Botton, "Self-organization of organoids from endoderm-derived cells," J. Mol. Med. **99**, 449–462 (2021).
[14]B. L. Strand, A. E. Coron, and G. Skjak-Braek, "Current and future perspectives on alginate encapsulated pancreatic islet stem cells," Transl. Med. **6**, 1053–1058 (2017).
[15]K. Alessandri, B. R. Sarangi, V. V. Gurchenkov, B. Sinha, T. R. Kießling, L. Fetler, F. Rico, S. Scheuring, C. Lamaze, A. Simon, S. Geraldo, D. Vignjević, H. Doméjean, L. Rolland, A. Funfak, J. Bibette, N. Bremond, and P. Nassoy, "Cellular capsules as a tool for multicellular spheroid production and for investigating the mechanics of tumor progression *in vitro*," Proc. Natl. Acad. Sci. U.S.A. **110**, 14843–14848 (2013).
[16]T. Kageyama, H. Akieda, Y. Sonoyama, K. Sato, H. Yoshikawa, H. Isono, M. Hirota, H. Kitajima, Y. S. Chun, S. Maruo, and J. Fukuda, "Bone beads enveloped with vascular endothelial cells for bone regenerative medicine," Acta Biomater. **165**, 168–179 (2023).
[17]M. E. Dolega, F. Abeille, N. Picollet-D'hahan, and X. Gidrol, "Controlled 3D culture in Matrigel microbeads to analyze clonal acinar development," Biomaterials **52**, 347–357 (2015).
[18]B. Sun, "The mechanics of fibrillar collagen extracellular matrix," Cell Rep. Phys. Sci. **2**, 100515 (2021).
[19]E. Mauri, I. Moroni, L. Magagnin, M. Masi, A. Sacchetti, and F. Rossi, "Comparison between two different click strategies to synthesize fluorescent nanogels for therapeutic applications," React. Funct. Polym. **105**, 35–44 (2016).
[20]N. Akhlaghi, S. Riahi, and R. Parvaneh, "Interfacial tension behavior of a nonionic surfactant in oil/water system; salinity, pH, temperature, and ionic strength effects," J. Pet. Sci. Eng. **198**, 108177 (2021).
[21]M. E. Mahmood and D. A. Al-Koofee, "Effect of temperature changes on critical micelle concentration for tween series surfactant effect of temperature changes on critical micelle concentration for tween series surfactant type: GJSFR-B," Chemistry **13**(4), 1–7 (2013).
[22]S. Yoshida, M. Takinoue, E. Iwase, and H. Onoe, "Dynamic transformation of self-assembled structures using anisotropic magnetized hydrogel microparticles," J. Appl. Phys. **120**, 084905 (2016).
[23]F. Davarcı, D. Turan, B. Ozcelik, and D. Poncelet, "The influence of solution viscosities and surface tension on calcium-alginate microbead formation using dripping technique," Food Hydrocoll. **62**, 119–127 (2017).
[24]L. Liu and G.-P. Shi, "CD31: Beyond a marker for endothelial cells," Cardiovasc. Res. **94**, 3–5 (2012).
[25]Y. Morimoto, Y. Tsuda, and S. Takeuchi, "Reconstruction of 3D hierarchic micro-tissues using monodisperse collagen microbeads," in *Proceedings of the IEEE International Conference on Micro Electro Mechanical Systems (MEMS)* (IEEE, 2009), pp. 56–59.
[26]B. van Loo, S. A. ten Den, N. Araújo-Gomes, V. de Jong, R. R. Snabel, M. Schot, J. M. Rivera-Arbeláez, G. J. C. Veenstra, R. Passier, T. Kamperman, and J. Leijten, "Mass production of lumenogenic human embryoid bodies and functional cardiospheres using in-air-generated microcapsules," Nat. Commun. **14**, 1–15 (2023).
[27]T. C. Martinsen, R. Fossmark, and H. L. Waldum, "The phylogeny and biological function of gastric juice—Microbiological consequences of removing gastric acid," Int. J. Mol. Sci. **20**, 6031 (2019).
[28]L. A. Miller, "Fluid dynamics of ventricular filling in the embryonic heart cell," Biochem. Biophys. **61**, 33–45 (2011).
[29]R. O. Hynes, "Integrins: Bidirectional, allosteric signaling machines," Cell **110**, 673–687 (2002).
[30]H. Svozilova, L. Vojtova, J. Matulova, J. Bruknerova, V. Polakova, L. Radova, M. Doubek, K. Plevova, and S. Pospisilova, "*In vitro* culture of leukemic cells in collagen scaffolds and carboxymethyl cellulose-polyethylene glycol gel," PeerJ **12**, e18637 (2024).
[31]S. Itai, H. Tajima, and H. Onoe, "Double-layer perfusable collagen microtube device for heterogeneous cell culture," Biofabrication **11**, 015010 (2018).
[32]Y. R. Lewis-Israeli, A. H. Wasserman, M. A. Gabalski, B. D. Volmert, Y. Ming, K. A. Ball, W. Yang, J. Zou, G. Ni, N. Pajares, X. Chatzistavrou, W. Li, C. Zhou, and A. Aguirre, "Self-assembling human heart organoids for the modeling of cardiac development and congenital heart disease," Nat. Commun. **12**(1), 5142 (2021).
[33]C. Schmidt, A. Deyett, T. Ilmer, A. T. Caballero, S. Haendeler, L. Pimpale, M. A. Netzer, L. C. Ginistrelli, M. Cirigliano, E. J. Mancheno, D. Reumann, K. Tavernini, S. Hering, P. Hofbauer, and S. Mendjan, "Multi-chamber cardioids unravel human heart development and cardiac defects," bioRxiv 2022.07.14.499699 (2022).
[34]J. Lee, A. Sutani, R. Kaneko, J. Takeuchi, T. Sasano, T. Kohda, K. Ihara, K. Takahashi, M. Yamazoe, T. Morio, T. Furukawa, and F. Ishino, "*In vitro* generation of functional murine heart organoids via FGF4 and extracellular matrix," Nat. Commun. **11**, 4283 (2020).
[35]P. Hofbauer, S. M. Jahnel, N. Papai, M. Giesshammer, A. Deyett, C. Schmidt, M. Penc, K. Tavernini, N. Grdseloff, C. Meledeth, L. C. Ginistrelli, C. Ctortecka, Š. Šalic, M. Novatchkova, and S. Mendjan, "Cardioids reveal self-organizing principles of human cardiogenesis," Cell **184**, 3299–3317.e22 (2021).
[36]A. Yaqinuddin, A. Jabri, A. Mhannayeh, B. Taftafa, M. Alsharif, T. Abbad, J. Khan, A. Elsalti, R. Chinnappan, E. A. Alshehri, A. Alzhrani, D. A. Obeid, I. Fujitsuka, M. Khan, M. Rehman, and T. A. Mir, "Cardiac organoids: A new tool for disease modeling and drug screening applications," Front. Cardiovasc. Med. **12**, 1537730 (2025).